Coordination between the actin cytoskeleton and membrane deformation by a novel membrane tubulation domain of PCH proteins is involved in endocytosis

Kazuya Tsujita, Shiro Suetsugu, Nobunari Sasaki, Masahiro Furutani, Tsukasa Oikawa, and Tadaomi Takenawa

Department of Biochemistry, Institute of Medical Science, University of Tokyo, Shirokanedai, Minato-ku, Tokyo, 108-8639 Japan

The conserved FER-CIP4 homology (FCH) domain is found in the pombe Cdc15 homology (PCH) protein family members, including formin-binding protein 17 (FBP17). However, the amino acid sequence homology extends beyond the FCH domain. We have termed this region the extended FC (EFC) domain. We found that FBP17 coordinated membrane deformation with actin cytoskeleton reorganization during endocytosis. The EFC domains of FBP17, CIP4, and other PCH protein family members show weak homology to the Bin-amphiphysin-Rvs (BAR) domain. The EFC domains bound strongly to phosphatidylserine and phosphatidylinositol 4,5-bisphosphate and deformed the plasma membrane and liposomes into narrow tubules. Most PCH proteins possess an SH3 domain that is known to bind to dynamin and that recruited and activated neural Wiskott-Aldrich syndrome protein (N-WASP) at the plasma membrane. FBP17 and/or CIP4 contributed to the formation of the protein complex, including N-WASP and dynamin-2, in the early stage of endocytosis. Furthermore, knockdown of endogenous FBP17 and CIP4 impaired endocytosis. Our data indicate that PCH protein family members couple membrane deformation to actin cytoskeleton reorganization in various cellular processes.

Introduction

Endocytic proteins such as dynamin, amphiphysin, and epsin, which directly bind and deform liposomes into tubules in vitro, play critical roles in membrane fission and curvature during clathrin-mediated endocytosis (Takei et al., 1999; Hinshaw, 2000; Itoh et al., 2001; Razzaq et al., 2001; Ford et al., 2002; Peter et al., 2004; Praefcke and McMahon, 2004). Dynamin is required for some forms of clathrin-independent or caveolae-mediated endocytosis (Praefcke and McMahon, 2004). These proteins interact directly with membrane phosphoinositides via lipid-binding domains, such as the pleckstrin homology (PH) domain in dynamin, the Bin-amphiphysin-Rvs (BAR) domain in amphiphysin, and the epsin NH_2-terminal homology (ENTH) domain in epsin. The BAR domain is proposed to drive membrane curvature (Peter et al., 2004).

The actin cytoskeleton is critical for many fundamental cellular processes such as cell morphology, motility, and cytokinesis (Pollard and Borisy, 2003; Rodriguez et al., 2003). Growing evidence indicates that the actin cytoskeleton plays an important role in endocytosis (Qualmann et al., 2000; Schafer, 2002; Engqvist-Goldstein and Drubin, 2003; Kaksonen et al., 2003). Actin regulatory proteins such as neural Wiskott-Aldrich syndrome protein (N-WASP), cortactin, and Abp1 bind to endocytic proteins such as syndapin, dynamin, and intersectin and are recruited to endocytic active zones (Qualmann and Kelly, 2000; Hussain et al., 2001; Kessels et al., 2001; Kessels and Qualmann, 2002; Cao et al., 2003; Otsuki et al., 2003). However, the role of the actin cytoskeleton in endocytosis is poorly understood. Recent work has revealed that both invagination and scission of clathrin-coated vesicles and local actin polymerization are highly coordinated, resulting in the efficient formation of coated vesicles (Merrifield et al., 2002, 2005).

The FER-CIP4 homology (FCH) domain is found in the pombe Cdc15 homology (PCH) family protein members and

Correspondence to Tadaomi Takenawa: takenawa@ims.u-tokyo.ac.jp

Abbreviations used in this paper: BAR, Bin-amphiphysin-Rvs; cDNA, complementary DNA; EFC, extended FC; ENTH, epsin NH_2-terminal homology; FBP17, formin-binding protein 17; FCH, FER-CIP4 homology; N-WASP, neural Wiskott-Aldrich syndrome protein; PC, phosphatidylcholine: PCH, pombe Cdc15 homology; PE, phosphatidylethanolamine; PH, pleckstrin homology; PI, phosphatidylinositol; PI(4,5)P2, phosphatidylinositol 4,5-bisphosphate; PS, phosphatidylserine; PSTPIP, proline-serine-threonine phosphatase–interacting protein; RNAi, RNA interference; siRNA, small interfering RNA; SH3, Src homology 3.

The online version of this article contains supplemental material.

The Journal of Cell Biology, Vol. 172, No. 2, January 16, 2006 269–279
http://www.jcb.org/cgi/doi/10.1083/jcb.200508091

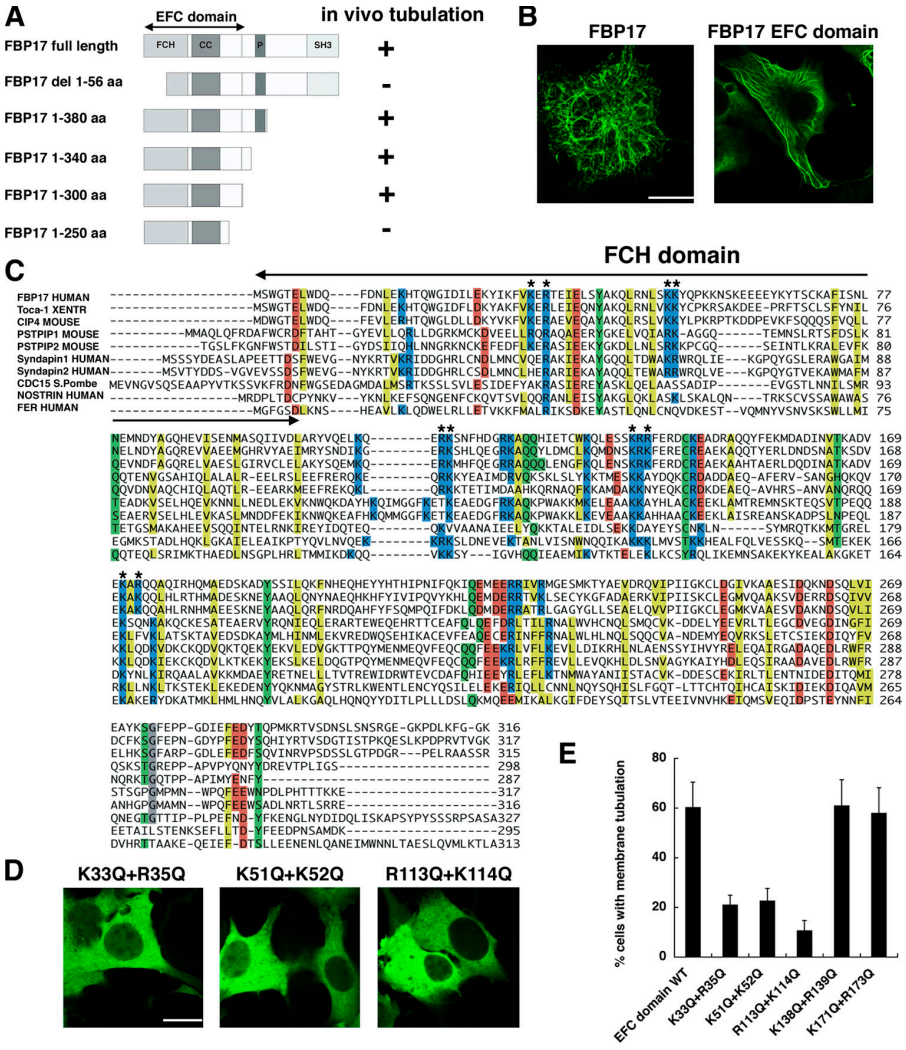

Figure 1. **Identification of functional EFC domain.** (A) Domain structures of FBP17 and deletion constructs. CC, coiled–coil; P, proline-rich motif. Tubulation ability is also indicated. (B) COS-7 cells were transfected with GFP-tagged FBP17 or GFP-tagged FBP17 1–300 aa, and GFP-fluorescence was observed by confocal microscopy. Bar, 20 μm. (C) Sequence alignment of the EFC domain. This alignment was obtained by Clustal W (Thompson et al., 1997). Conserved residues are highlighted with the following color code: yellow, hydrophobic; green, polar; blue, basic; red, acidic. Asterisks show the mutation sites. (D) Effect of the GFP-tagged K33Q + R35Q, K51Q + K52Q, R113Q + K114Q and mutants of the EFC domain of FBP17 on tubulation in COS-7 cells. Bar, 20 μm. (E) 50 cells overexpressing GFP-tagged K33Q + R35Q, K51Q + K52Q, R113Q + K114Q, K138Q + K139Q, and K171Q + R173Q mutants scored for tabulation. the results are presented as percentages. Three independent experiments were performed. All error bars indicate SEM.

is highly conserved from yeast to mammals (Aspenstrom, 1997; Lippincott and Li, 2000). Most PCH proteins have the Src homology 3 (SH3) domain at the COOH terminus. PCH family members, including CIP4; formin-binding protein 17 (FBP17); Toca-1; syndapins/PACSINs; cdc15; and proline-serine-threonine phosphatase–interacting proteins (PSTPIPs), are known to be involved in cytoskeletal and endocytic events (Fankhauser et al., 1995; Spencer et al., 1997; Modregger et al. 2000; Qualmann and Kelly, 2000; Kamioka et al., 2004; Ho et al., 2004; Chitu et al., 2005). Syndapins/PACSINs and FBP17 are implicated in endocytosis by their abilities to bind to dynamin via their SH3 domain (Qualmann and Kelly, 2000; Kamioka et al., 2004). In particular, FBP17 induces tubular membrane invagination, suggesting that this protein generates the membrane curvature necessary for dynamin-dependent endocytosis (Kamioka et al., 2004). In this regard, syndapins/PACSINs have been predicted to be potential BAR domain–containing proteins (Peter et al., 2004).

Interestingly, several PCH family members have been shown to bind to both WASP/N-WASP and dynamin, indicating that the PCH family is involved in actin cytoskeleton reorganization associated with membrane fission or protrusion (Qualmann and Kelly, 2000; Ho et al., 2004; Kakimoto et al., 2004). All PCH proteins possess a highly conserved region that includes and extends beyond the FCH domain. The conserved region includes a predicated coiled–coil region, suggesting that this region is a novel functional domain. However, the exact functions of this region are unknown. We term this region the extended FC (EFC) domain and show that the EFC domain binds to phosphatidylserine (PS) and phosphatidylinositol 4,5-bisphosphate (PI[4,5]P2). The EFC domain shows weak homology to the BAR domain, and the EFC domain alone tubulates liposomes in vitro. Importantly, the EFC domain–containing protein FBP17 is directly involved in EGF internalization, including plasma membrane invagination and actin polymerization, via recruitment of dynamin-2 and N-WASP.

Results

Identification of functional EFC domain

Expression of FBP17 has been shown to induce plasma membrane tubulation in COS-1 cells (Kamioka et al., 2004). We identified the specific domain of FBP17 critical for membrane tubulation. By expression analysis of various deletion constructs in COS-7 cells, we found that 1–300 aa, comprising a sequence longer than the FCH domain, is required for membrane tubulation

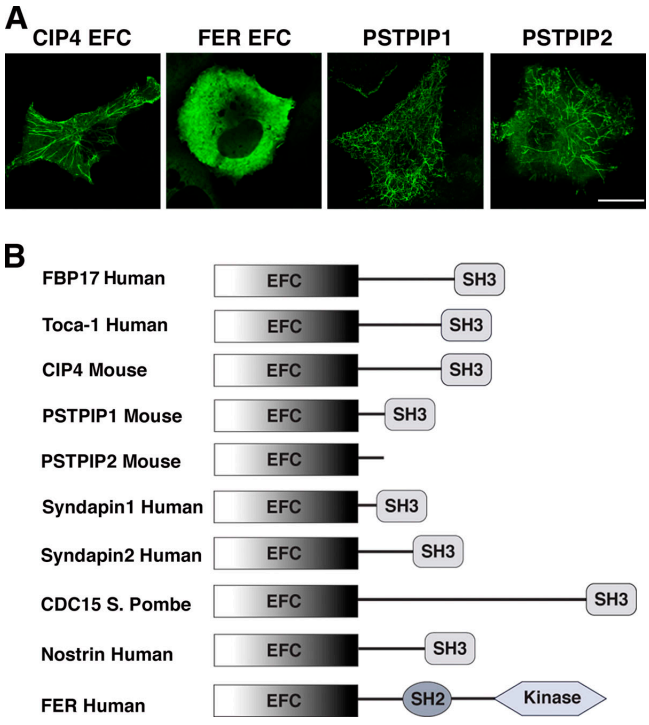

Figure 2. **EFC domain in other proteins.** (A) In vivo tubulation by overexpression of the GFP-tagged CIP4 EFC domain, GFP-tagged FER EFC domain, GFP-tagged PSTPIP1, and GFP-tagged PSTPIP2 in COS-7 cells. Bar, 20 μm. (B) The domain organization of the EFC domain–containing protein.

(Fig. 1 A). Expression of 1–300 aa, but not of 1–250 aa, deformed membranes into tubules that were longer than those induced by the full-length protein (Fig. 1, A and B).

Alignment of these sequences in FCH domain–containing proteins revealed that the sequence homology extended beyond the FCH domain and included a predicated coiled–coil region of ~100–200 aa (Fig. 1 C and Fig. S1, available at http://www.jcb.org/cgi/content/full/jcb.200508091/DC1). Interestingly, this region showed weak homology to the BAR domain (Fig. S1). Residues inside of the helix packing of the BAR domain are well conserved (Peter et al., 2004; Fig. S1). As expected, the coiled–coil region contributed to dimer formation of this region as determined by chemical cross-linking analysis (unpublished data). The basic amino acid residues of the BAR and the ENTH domain are essential for binding and tubulation of liposomes (Itoh et al., 2001; Ford et al., 2002; Peter et al., 2004). To determine if the basic amino acid residues of this extended domain are involved in the binding to liposomes, we performed mutagenesis analysis. Some sites composed of basic residues are conserved in the extended domain (Fig. 1 C). Therefore, we mutated these basic amino acid to Gln. Interestingly, expression of the K33Q + R35Q, K51Q + K52Q, or R113Q + K114Q mutant did not induce membrane tubulation in cells compared with that of wild-type extended domain (Fig. 1, D and E). In contrast, the K138Q + R139Q or K171Q + R173Q mutant induced tubulation similar to that of the wild-type extended domain (Fig. 1 E).

Expression of other PCH proteins including CIP4 (1–300 aa), PSTPIP1 (1–415 aa), and PSTPIP2 (1–337 aa) also resulted in membrane tubulation in cells (Fig. 2 A). However, expression of FER (aa 1–300) resulted in little tubulation (Fig. 2 A). In FER, amino acid residues corresponding to K33, K51, and K52 of FBP17 are not conserved, but those corresponding to R113 and K114 are conserved (Fig. 1 C). K33 and K51, but not R113/R114, are conserved between the BAR domain and the extended domain (Fig. S1). The relation between sequence conservation and tubulation ability indicates that this region is evolutionally and functionally conserved and is related to the BAR domain. Because a portion of this region includes the FCH domain, we termed the entire conserved region the EFC domain, which is located at the NH_2 terminus (Fig. 2 B).

The EFC domain is a novel phosphoinositide-binding module

We next examined whether the EFC domain can bind to lipids because domains that deform membrane interact directly with membrane lipids (Peter et al., 2004). We performed liposome sedimentation assays and found that the EFC domain of FBP17 bound most strongly to PI(4,5)P2-containing liposomes (Fig. 3, A and B). Brain lipids (Folch fraction) or PI(3,4,5)P3 also bound moderately to the EFC domain. Brain lipids are rich in PS (~50% of total lipids), and the EFC domain of FBP17 bound to PS-containing liposomes (Fig. 3, A and B). However, it did not bind to lysophosphatidic acid, lysophosphocholine, or sphingosine-1-phosphate (unpublished data). The dissociation constant (K_d) of the EFC domain for PI(4,5)P2 binding was determined with a dual polarization interferometer and was found to be 395.3 nM, comparable to those of the PLCδ1 PH and the epsin ENTH domains, which are known to bind PI(4,5)P2 with high affinity (Itoh et al., 2001; Ford et al., 2002; Fig. 3 C).

We then tested whether the tubulation activity of the EFC domain in cells correlates with its lipid-binding ability. Mutants with reduced tubulation activity showed decreased lipid-binding ability compared with that of wild-type EFC, indicating that direct interaction with phosphoinositides is necessary for membrane tubulation in cells (Fig. 3 D). The EFC domains of other proteins also bound to PI(4,5)P2. For example, the EFC domains of CIP4, FER, PSTPIP1, and PSTPIP2 also bound strongly to PI(4,5)P2 and to brain lipids (Fig. 3 E). These results indicate that the lipid-binding ability of the EFC domain is evolutionally conserved and that the EFC domain comprises a novel phosphoinositide-binding module.

The EFC domain alone tubulates protein-free liposomes in vitro

Expression of the EFC domain strongly induced membrane tubulation in cells, and it showed high affinity for phosphoinositides. We next examined whether it can deform artificial liposomes composed of brain or synthetic lipids, including PI(4,5)P2. The PLCδ1 PH domain, which binds to PI(4,5)P2 with high affinity, did not alter the shape of brain liposomes (Fig. 4 A). In contrast, the EFC domain of FBP17 induced tubulation of brain liposomes (Fig. 4 A), as did the BAR domain of amphiphysin2/Bin1 (Amph2; Razzaq et al., 2001; Lee et al., 2002). The tubulation of liposomes by the EFC domain and by the BAR domain was confirmed by electron microscopy (Fig. 4 B).

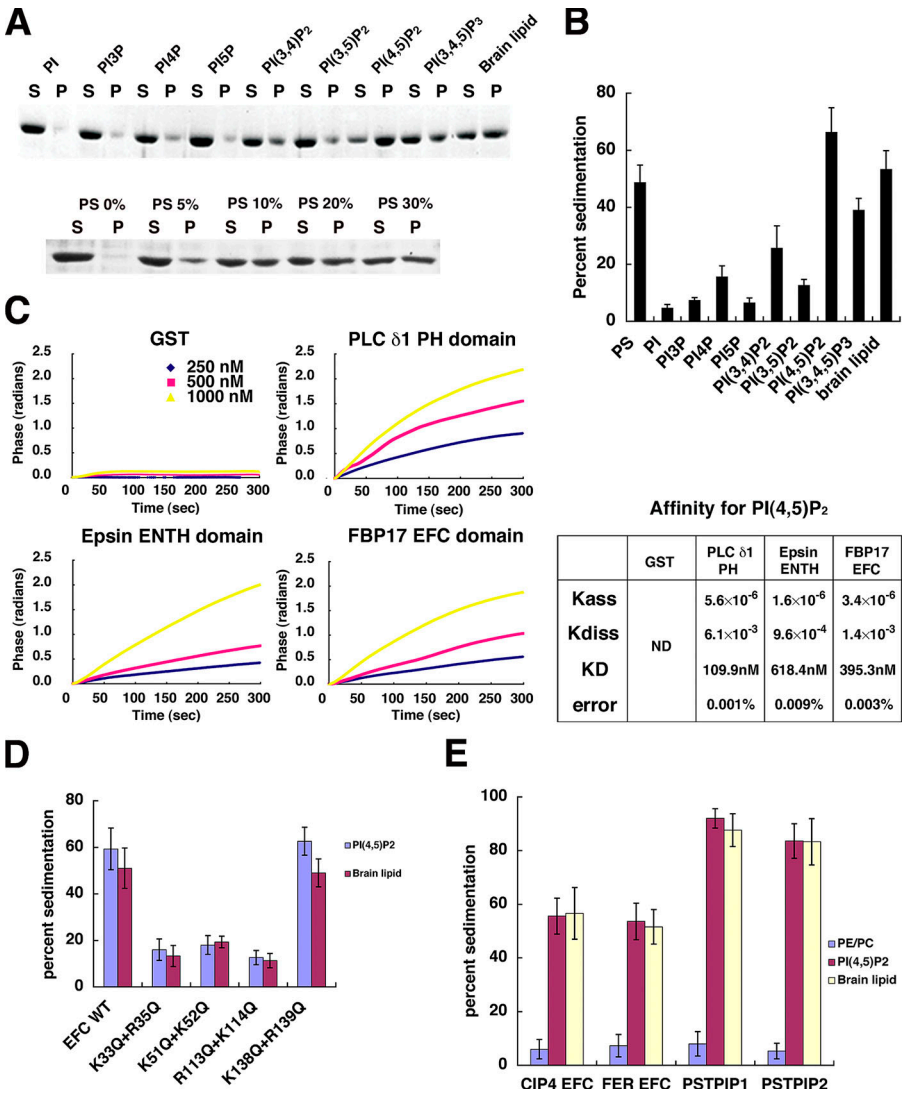

Figure 3. **The EFC is a novel phosphoinositide binding module.** (A) The EFC domain of FBP17 strongly bound to PS and PI(4,5)P2. (top) Brain lipid (Folch lipid) or synthetic PE/PC liposomes supplemented with 10% of the indicated lipid were incubated with the EFC domain and sedimented, and then stained with Coomassie brilliant blue. (bottom) Synthetic PE/PC liposomes supplemented with various percentages of PS were also analyzed. S, supernatant; P, pellet. (B) Quantitative representation of A. Three independent experiments were performed and the protein band intensity was measured. (C) The dissociation constant (K_d) of the indicated domain for PI(4,5)P2 was determined using dual polarization interferometer. The response curves (left) used for the calculation of K_d (right) were shown. (D) Comparison of the lipid binding of wild type and mutants of the FBP17 EFC domain examined by sedimentation assay. Three independent experiments were performed. (E) Sedimentation assays with the EFC domain of CIP4 and FER, or PSTPIP1 and PSTPIP2, to examine the association with lipids. Three independent experiments were performed. All error bars indicate SEM.

The diameter of tubules induced by the EFC domain of FBP17 (~200 nm) was larger than that of tubules induced by the BAR domain of Amph2 (~50 nm; Peter et al., 2004). Because the EFC domain bound strongly to PI(4,5)P2, it was incubated with PI(4,5)P2-supplemented brain liposomes (although brain lipids themselves contain a small amount of PI[4,5]P2). Increased PI(4,5)P2 concentration enhanced the tubulation of brain lipids by the EFC domain; very long liposome tubules, up to ~60 μm in length, were formed upon the addition of PI(4,5)P2 (Fig. 4 C).

To confirm the involvement of PI(4,5)P2 on liposome tubulation by the EFC domain, we performed a series of experiments. The EFC domain did not induce tubulation of synthetic liposomes composed of phosphatidylethanolamine (PE)/phosphatidylcholine (PC)/phosphatidylinositol (PI) (Fig. 4 C). Addition of PI(4,5)P2 to these liposomes reenabled the ability of the EFC domain to induce the tubulation (Fig. 4 C). Interestingly, addition of the PLCδ1 PH domain at a one- or threefold molar excess to that of the EFC domain decreased liposome tubulation by the EFC domain (Fig. 4 D). Furthermore, overexpression of the PLCδ1PH domain in cells strongly inhibited the tubulation (Fig. 4 E), whereas high concentrations of wortmannin, which is a PI 3-kinase inhibitor, did not affect tubulation at all (not depicted). Because the PLCδ1PH domain competed with the EFC domain, these data indicate that the binding of the EFC domain to PI(4,5)P2 may enhance the membrane tubulation in cells and in vitro.

We next examined the liposome tubulation by EFC mutants defective in the plasma membrane tubulation in cells. The K33Q + R35Q, K51Q + K52Q, and R113Q + K114Q mutants, which showed reduced lipid-binding ability, induced little tabulation (Fig. 4 F).

In addition, the EFC domains of CIP4 and PSTPIP1 strongly induced liposome tubulation (Fig. 4 G). The EFC domain of FER also induced tubulation; however, the efficiency was less than that of other EFC domains (Fig. 4 G). Decreased tubulation in vitro may reflect the lack of tubulation in cells expressing the EFC domain of FER (Fig. 2 A). These data indicate that the EFC domain alone can induce membrane tubule formation by interacting directly with the lipid bilayer.

FBP17 is required for endocytosis of EGF

FBP17 is thought to play a role in endocytosis (Kamioka et al., 2004). Therefore, we studied the involvement of the EFC

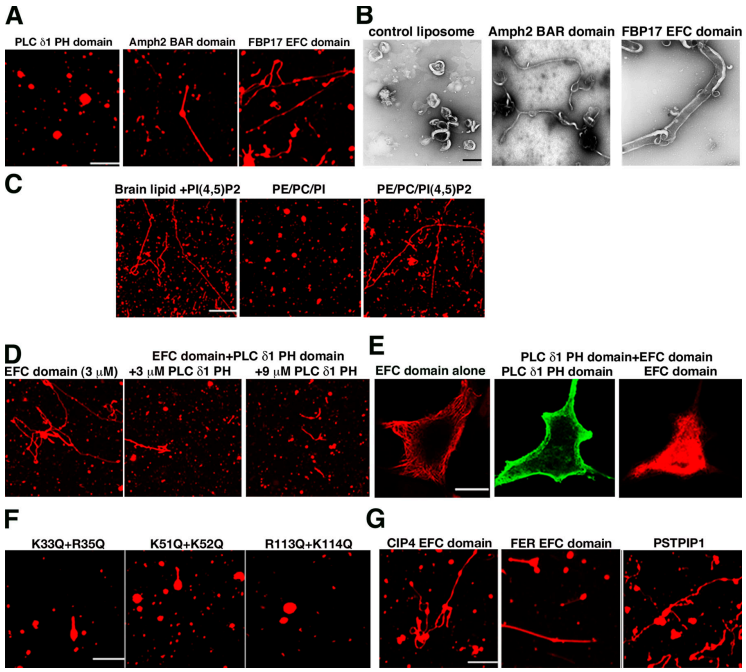

Figure 4. **The EFC domain alone tubulates protein-free liposomes in vitro.** (A) Brain lipid liposomes containing 5% rhodamine-conjugated PE (rhodamine-PE) were incubated with the PLCδ1 PH domain, amphiphysin2/Bin 1 BAR domain, or FBP17 EFC domain and examined by confocal microscopy. Bar, 5 μm. (B) Brain lipid liposomes were incubated with Amph2 BAR domain or FBP17 EFC domain and examined by electron microscopy. Bar, 200 nm. (C) Brain lipid liposomes containing 5% rhodamine-PE and 10% PI(4,5)P2 or synthetic lipid liposomes containing 70% PE, 15% PC, 5% rhodamine-PE, and either 10% PI, PI(4,5)P2, or PI(3,4,5)P3 were incubated with the EFC domain. Afterward, the liposomes were examined by confocal microscopy. Bar, 10 μm. (D) 3 μM of the EFC domain was incubated with brain lipid liposomes containing 5% of rhodamine-PE and 10% of PI(4,5)P2 as in C (left, EFC domain). The PLCδ1 PH domain (3 or 9 μM) was preincubated with these liposomes for 2 min, and then the liposomes were incubated with 3 μM of the EFC domain for 2 min and examined by confocal microscopy. (E) HA-tagged FBP17 EFC domain alone or with GFP-tagged PLCδ1 PH domain (green) was transfected into COS-7 cells. The EFC domain protein was visualized with anti-HA antibody (red). Bar, 20 μm. (F) Brain liposomes containing 5% rhodamine-PE and 10% PI(4,5)P2 were incubated with the K33Q + R35Q, K51Q + K52Q, and R113Q + K114Q mutant. Bar, 5 μm. (G) Brain lipid liposomes containing 5% of rhodamine-PE and 10% of PI(4,5)P2 were incubated with the EFC domain of CIP4, FER, or PSTPIP1. Bar, 5 μm.

domain of FBP17 in the endocytosis of EGF. The uptake of Texas red–labeled EGF was decreased in cells overexpressing FBP17 (Fig. 5 A). When we observed cells with strong FBP17 expression, Texas red–labeled EGF remained on the surface and associated with tubules, as reported previously (Kamioka et al., 2004). In contrast, EGF was internalized and observed as dots within the control cells (Fig. 5 A). Approximately 25% of FBP17-overexpressing cells showed a clear dots staining (Fig. 5 A, histogram). SH3 domain–deleted FBP17 also inhibited the endocytosis of EGF (Fig. 5 A). We next performed a quantitative assay that measures internalization of biotinylated EGF as a function of total bound biotinylated EGF. A small, but reproducible, reduction of internalization of EGF in total cells was observed upon expression of FBP17 under ~20–30% of transfection efficiency (Fig. 5 B). Interestingly, this decrease appeared to be dependent on the entire EFC domain because the 1–56-aa deletion mutant did not inhibit endocytosis (Fig. 5, A and B).

We next examined whether endogenous FBP17, CIP4, and Toca-1 are involved in endocytosis by RNA interference (RNAi) using small interfering RNA (siRNA). We confirmed that each siRNA selectively reduced the amount of FBP17 mRNA, Toca-1 mRNA, or CIP4 protein. (Fig. 5 C). In cells with reduced FBP17 or CIP4 expression, the uptake of Texas red–labeled EGF was reduced compared with that in cells treated with control siRNA by microscopic analysis (Fig. 5 D). Moreover, double depletion of FBP17 and CIP4 further reduced EGF internalization (Fig. 5 D). We next performed a quantitative assay that measures internalization of biotinylated EGF as a function of total bound biotinylated EGF. Cells with reduced FBP17 or CIP4 expression exhibited reduced EGF internalization compared with cells treated with control RNAi (Fig. 5 E). However, reduction of Toca-1 expression proved less effective. Double depletion of FBP17 and CIP4 more effectively reduced EGF internalization (Fig. 5 E). Importantly, decreased EGF internalization in response to RNAi treatment began after 5 min of EGF application to cells, indicating that these proteins are involved in the early steps of endocytosis. These data suggest that FBP17 and CIP4 play redundant roles in EGF internalization.

FBP17 recruits N-WASP to the plasma membrane, where it activates actin polymerization

Recent studies have shown that FBP17 binds to dynamin-2 and to N-WASP (Kamioka et al., 2004; Kakimoto et al., 2004), both of which play important roles in endocytosis (Kessels and Qualmann, 2002; Otsuki et al., 2003; Merrifield et al., 2004; Praefcke and McMahon, 2004). Therefore, we examined whether FBP17 is colocalized with dynamin-2 and/or N-WASP. FBP17 that was expressed at a low level hardly induced tubulation. Instead, low-expressed

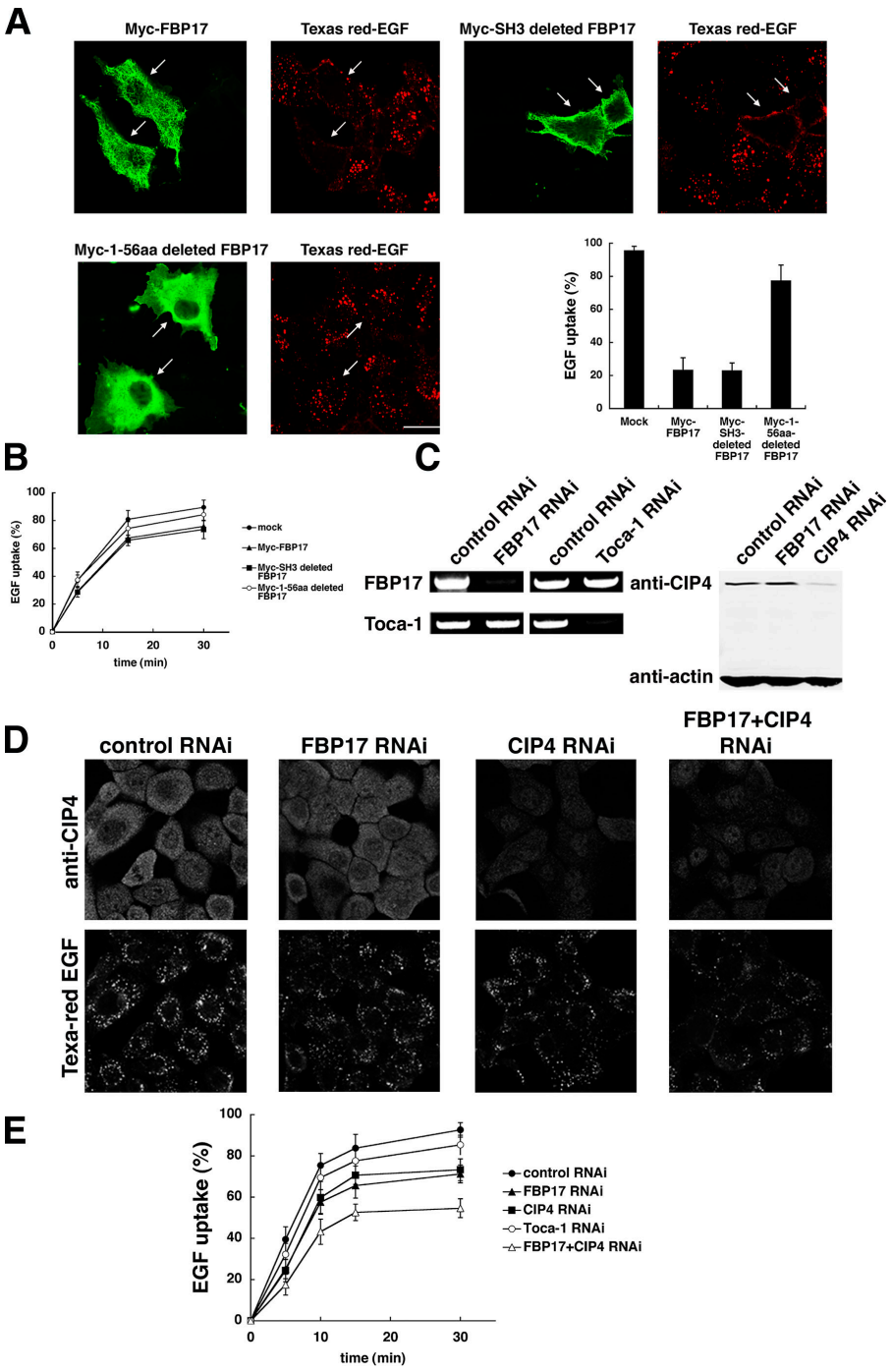

Figure 5. **FBP17 is required for endocytosis of EGFR.** (A) Myc-tagged wild-type FBP17, SH3 domain–deleted FBP17, and 1–56 aa–deleted FBP17 were transfected in COS-7 cells. After starvation for 16 h, the transfected cells were incubated with Texas red–EGF (red) for 15 min, fixed, and stained with anti-Myc antibody (green). The percentage of cells with internalized EGF among FBP17-overexpressing cells was also shown with SD. Bar, 20 μm. (B) Quantitative EGF internalization assay of FBP17-transfected cells. The histogram shows uptake of biotinylated EGF as a function of total bound biotinylated EGF at indicated times in transfected cells. Data from three independent experiments. Error bars represent SD. (C) A431cells were transfected with the control, FBP17, CIP4, and Toca-1siRNA. After 24 h, a second transfection was performed and the cells were cultured for an additional 72 h and subjected to RT-PCR and Western blotting. (D) After 96 h, the cells transfected with the siRNA were incubated with Texas red-EGF for 10 min, fixed, and stained with anti-CIP4 antibody. (E) Quantitative EGF internalization assay of siRNA-transfected cells as in B. Data from three independent experiments. All error bars indicate SEM.

FBP17 was localized to the plasma membrane of COS-7 cells in a punctate pattern (Fig. 6 A and Fig. S2, A and B, available at http://www.jcb.org/cgi/content/full/jcb.200508091/DC1). FBP17 colocalized with dynamin-2 at the plasma membrane (Fig. S2 A). Moreover, FBP17 colocalized with EGF at the plasma membrane before the recruitment of Rab5, which is a marker protein for clathrin-coated vesicles/early endosomes (Zerial and McBride, 2001; Fig. S2 B), indicating that FBP17 functions in the early endocytic events, such as invagination. Importantly, FBP17 also colocalized with N-WASP at the plasma membrane at sites where actin polymerization was induced (Fig. 6 A). N-WASP is known to activate the Arp2/3 complex to induce actin polymerization. FBP17 also colocalized with Arp2 only at the cell periphery (Fig. 6 B). The SH3 domain of several EFC domain–containing proteins has been reported to bind to N-WASP (Qualmann and Kelly, 2000; Ho et al., 2004; Kakimoto et al., 2004). The SH3-deleted FBP17 that was expressed at a low level was localized to the plasma membrane in a manner similar to wild-type FBP17, but did not colocalize with N-WASP, and actin polymerization was no longer observed (Fig. 6 C). Thus, FBP17 may function in endocytosis as an N-WASP activator, inducing actin polymerization via activation of the Arp2/3 complex.

We next examined whether FBP17 activates the N-WASP–Arp2/3 complex, leading to actin polymerization. FBP17

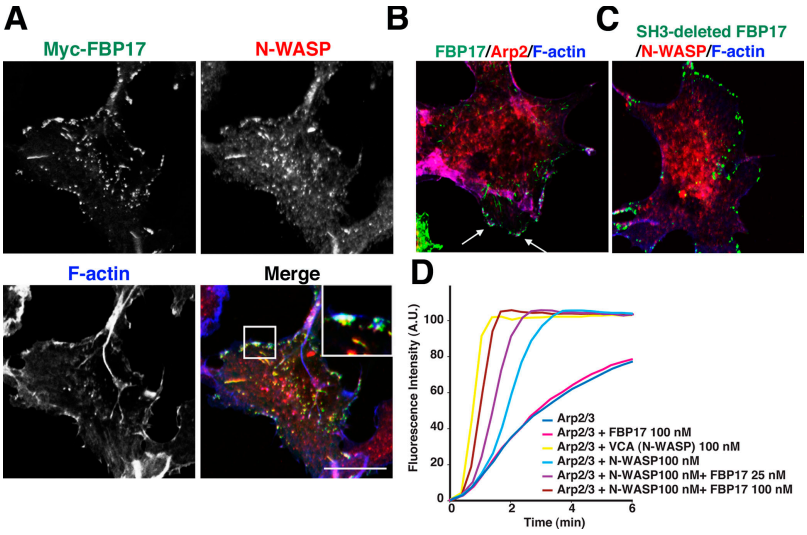

Figure 6. **FBP17 recruits N-WASP to plasma membrane where it activates actin polymerization.** (A) Myc-tagged FBP17 was transfected in COS-7 cells. The cells were stained with anti-Myc antibody (green) and anti–N-WASP antibody (red), and incubated with Alexa Fluor 647–conjugated phalloidin (blue) for visualization of actin filaments. Cells with expression of FBP17 at a low level is shown. Bar, 20 μm. (B) Myc-tagged FBP17 transfected in COS-7 cells were stained with anti-Myc antibody (green) and anti-Arp2 antibody (red) and incubated with Alexa Fluor 647–conjugated phalloidin (blue). (C) Myc-tagged SH3 domain–deleted FBP17 was transfected into COS-7 cells and the cells were stained by the same method as in A. (D) In vitro actin polymerization assay was performed with 0.2 μM of pyrene-labeled monomeric actin, 2 μM of unlabeled monomeric actin, 60 nM Arp2/3 complex, and 100 nM verprolin homology/cofilin homology/acidic region of N-WASP or 100 nM N-WASP, with or without GST-tagged FBP17 at various concentrations.

activated the N-WASP–Arp2/3 complex–dependent actin polymerization in vitro (Fig. 6 D), supporting the notion that FBP17 recruits N-WASP to the plasma membrane via the SH3 domain and induces actin polymerization in an N-WASP–Arp2/3 complex–dependent manner.

The PCH protein family binds to N-WASP and dynamin-2

We examined the affinities of the SH3 domains of FBP17 and other PCH family proteins for N-WASP and dynamin-2. The SH3 domains of CIP4, FBP17, Toca-1, and PSTPIP1 bound to N-WASP and dynamin-2 (Fig. 7 A). In pull-down assays, N-WASP was more concentrated in SH3 domain precipitates than dynamin-2. (Fig. 7 B). The SH3 domains of CIP4, FBP17, Toca-1, and PSTPIP1 appear to bind to N-WASP and dynamin-2 in a similar manner. N-WASP and dynamin-2 form a protein complex in the early stage of endocytosis (Otsuki et al., 2003). FLAG-tagged N-WASP was expressed with or without GFP-tagged FBP17. The amount of dynamin-2 in anti-FLAG immunoprecipitates was significantly increased upon expression of FBP17 (Fig. 7 C), indicating that dimerized FBP17 physically links N-WASP and dynamin-2 (Fig. 7 B). However, many other proteins bind to the SH3 domains of these proteins (Fig. 7 A). These unidentified proteins may play important roles in regulating FBP17, CIP4, and Toca-1.

EGFR, dynamin-2, and N-WASP are associated with invaginating tubules induced by FBP17

We next examined the localization of proteins involved in endocytosis in membrane tubulated by FBP17. EGFR was colocalized with FBP17 in invaginating tubules (Fig. 8 A). N-WASP was also localized in these invaginating tubules, whereas SH3-deleted FBP17 was not colocalized with N-WASP, but still induced membrane tubulation (Fig. 8 B). Moreover, N-WASP colocalized with dynamin-2 in these tubules (Fig. 8 C). Combined with the immunoprecipitation analysis, these data indicate that these proteins are able to form a functional complex.

Actin polymerization and formation of FBP17-associated tubules

Recent studies have indicated that actin polymerization has critical roles in the fission of endocytic vesicles away from the plasma membrane (Kaksonen et al., 2003; Merrifield et al., 2005). Moreover, inhibition of actin polymerization increases deep invaginations at the plasma membrane (Yarar et al., 2005). Thus, we examined the relationship between actin polymerization and tubular invagination induced by FBP17. Overexpression of FBP17 induced tubules that did not merge with the actin

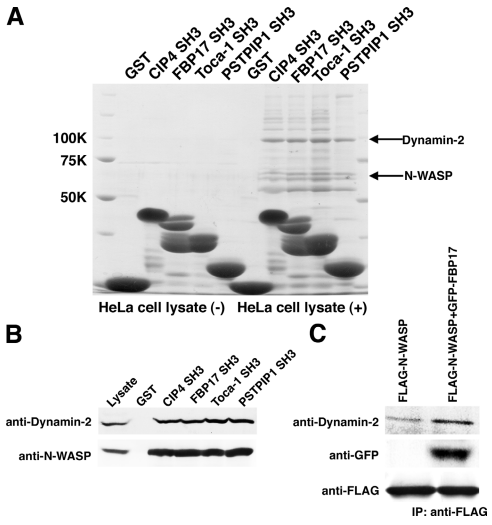

Figure 7. **The PCH proteins bind to N-WASP and dynamin-2 via the SH3 domain.** (A) The pull-down assay was shown. GST alone, or GST-CIP4 SH3 domain, GST-FBP17 SH3 domain, GST-Toca-1 SH3 domain, and PSTPIP1 SH3 domain were immobilized on glutathione–sepharose beads and incubated with HeLa cell lysate. After washing, each sample was subjected to SDS-PAGE analysis and stained with Coomassie brilliant blue. (B) Pull-down samples were analyzed by Western blotting with anti–Dynamin-2 antibody or anti–N-WASP antibody. (C) Immunoprecipitation analysis. The cells transfected with FLAG-tagged N-WASP and/or GFP tagged FBP17 were immunoprecipitated with anti-FLAG. Coprecipitation of Dynamin-2 was analyzed by Western blotting.

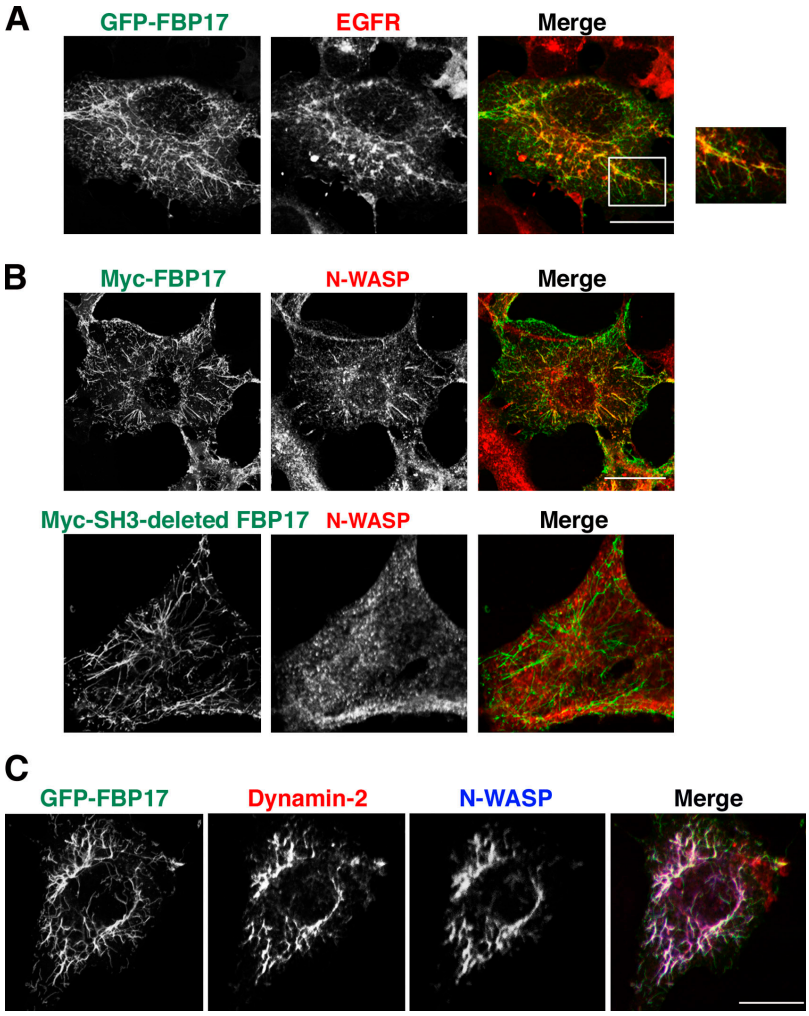

Figure 8. **EGFR, dynamin-2, and N-WASP are associated with invaginating tubules induced by FBP17.** (A) GFP-FBP17 was transfected in COS-7 cells. After starvation for 16 h, the transfected cells were stimulated with 100 ng/ml EGF for 15 min, fixed, and stained by anti-GFP (green) and anti-EGFR (red) antibodies. (B) Myc-tagged FBP17 and SH3 domain–deleted FBP17-transfected COS-7 cells were stained with anti-Myc (green) and anti–N-WASP (red) antibodies. Bar, 20 μm. (C) GFP-tagged FBP17 was transfected in COS-7 cells and stained with anti–dynamin-2 (red) and anti–N-WASP (blue) antibodies. Bar, 20 μm.

cytoskeleton (Fig. 9 A). Interestingly, coexpression of FBP17 and N-WASP, which is expected to strongly induce actin polymerization (Fig. 6 D), decreased the plasma membrane tubulation induced by FBP17 (Fig. 9, A and B). Instead, FBP17 localized in a punctate pattern at the plasma membrane, where it colocalized with N-WASP and cortical actin structure (Fig. 9 A). Importantly, the protein complex including dynamin-2 and N-WASP was observed upon expression of both N-WASP and FBP17 (Fig. 7 C). Tubules induced by the SH3-deleted FBP17 were not significantly attenuated by overexpression of N-WASP (Fig. 9 B). Consistently, inhibition of actin polymerization by treatment of latrunculin B increased FBP17-induced plasma membrane tubulation (unpublished data). Low-expressed FBP17 exhibited a punctate pattern of localization, but latrunculin B treatment caused the elongated tubular structures by low expressed FBP17 (Fig. 9, C and D). Therefore, the degree of actin polymerization downstream of FBP17 appears to be important for tubulation. Importantly, a previous paper pointed out the importance of dynamin in tubulation; mutants of dynamin defective in binding to FBP17 enhanced the tubulation (Kamioka et al., 2004). These data suggest that these tubules might be created by the deformation of endocytic vesicles, for which fission by the coordination of dynamin-2 and actin polymerization is required.

Discussion

In this study, we identified a novel domain, the EFC domain, which is related to the BAR domain. Half of the EFC domain was previously characterized as an FCH domain, but an additional sequence is required for interaction with the membrane. Our results provide the first evidence that the EFC domain of FBP17 directly binds to the membrane and deforms protein-free liposomes into tubules. Moreover, the EFC domains of other PCH family proteins, such as CIP4, FER, PSTPIP1, and PSTPIP2, also strongly bind to and tubulate liposomes (Figs. 3 and 4). Conservation of both amino acid sequence and function indicate that the EFC domain is a membrane tubulation module that is dependent on lipid binding.

The SH3 domain of FBP17 and that of other EFC domain–containing proteins bind to dynamin-2 and N-WASP. Dimerized FBP17 recruited N-WASP and dynamin-2 simultaneously (Figs. 7 and 8). N-WASP and dynamin preferentially bind to PI(4,5)P2 (Ho et al., 2004; Praefcke and McMahon, 2004). The EFC domain of FBP17 binds to PI(4,5)P2 preferentially (Fig. 3). Therefore, these proteins form a functional complex at the PI(4,5)P2-rich plasma membrane. Thus, FBP17 may provide links between membrane invagination, fission, and

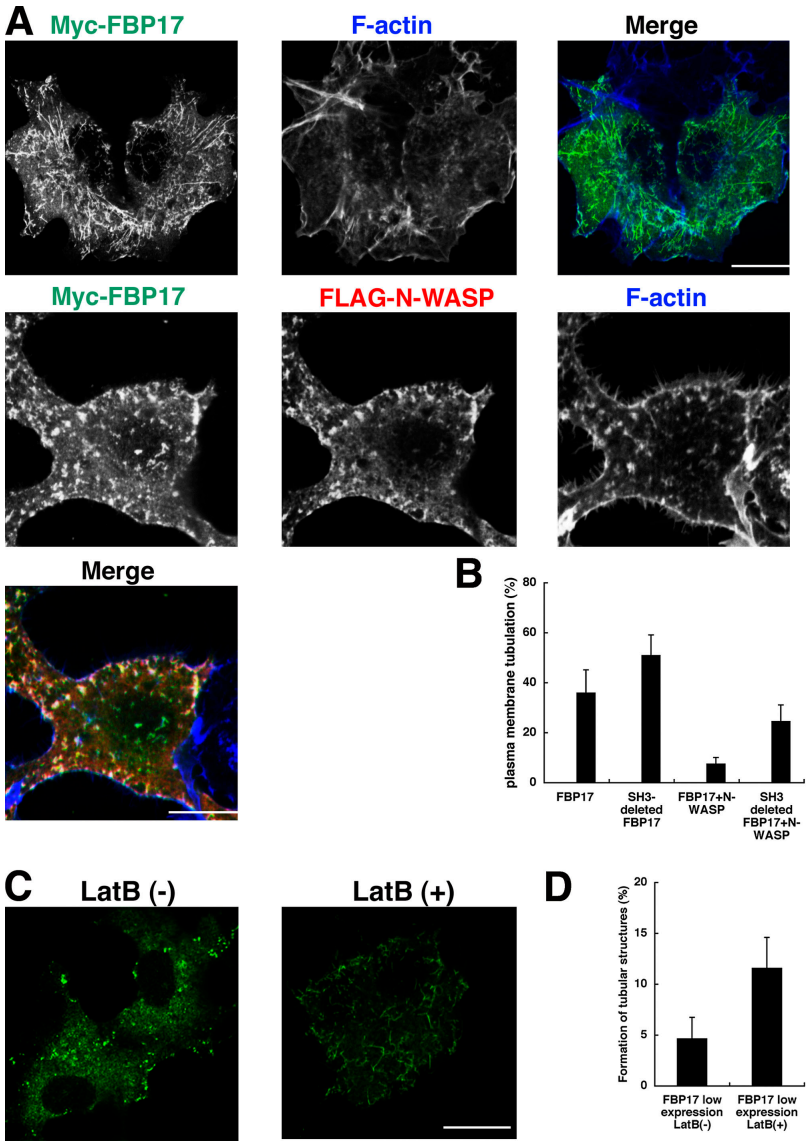

Figure 9. **Actin polymerization and formation of FBP17-associated tubules.** (A) Myc-tagged FBP17 alone or Myc-tagged FBP17 plus Flag-tagged N-WASP were transfected in COS-7 cells. The cells were stained with anti-Myc (green) antibody, anti–N-WASP antibody (red), and Alexa Fluor 647–conjugated phalloidin (blue). Bar, 20 μm. (B) Quantitative analysis of plasma membrane tubulation upon N-WASP overexpression. $n = 50$ cells. Three independent experiments were performed. Error bars represent SD. (C) GFP-FBP17 transfected COS-7 cells were treated with DMSO or latrunculin B (LatB; 5 μM) for 5 min. Bar, 20 μm. (D) Quantitative analysis of induction of tubular structures after latrunculin B treatment. $n = 50$ cells. Three independent experiments were performed. All error bars indicate SEM.

actin polymerization, mediated by FBP17, dynamin-2, and N-WASP, respectively (Fig. S3, available at http://www.jcb.org/cgi/content/full/jcb.200508091/DC1).

We found that FBP17 is required for EGF endocytosis by both knockdown and localization studies (Fig. S2 and Fig. 5). Importantly, both the EFC domain and the SH3 domain of FBP17 were required for the recruitment of N-WASP and dynamin-2 to the plasma membrane. Because tubulation induced by FBP17 expression is enhanced by decreasing the affinity of dynamin to FBP17 (Kamioka et al., 2004), and because increased amounts of N-WASP decreased tubulation (Fig. 9), the lack of appropriate binding partners for FBP17 may induce tabulation, presumably via the inhibition of fission of endocytic vesicles. Consistent with this idea, low-expressed FBP17 formed tubular structures when actin polymerization was blocked by latrunculin B treatment (Fig. 9, C and D). FBP17-induced tubulation was also enhanced by the inhibition of actin polymerization (unpublished data). The Arp2/3 complex was colocalized with FBP17-induced tubules only at the cell periphery (Fig. 6 B), also indicating that the lack of proper actin polymerization machinery caused the tubulation. Therefore, actin polymerization that occurs downstream of FBP17 may be essential for fission of endocytic vesicles, together with dynamin. Actually, the actin cytoskeleton is essential for the internalization step of endocytosis at the plasma membrane in yeast and mammals (Munn, 2001; Merrifield et al., 2002, 2005; Engqvist-Goldstein and Drubin, 2003). Dynamin plays an established role in the fission of endocytic vesicles (Takei et al., 1998; Hinshaw, 2000). Thus, imbalanced recruitment of dynamin-2 or of the actin polymerization machinery, including N-WASP, may induce the tubulation associated with FBP17 and other EFC domain–containing proteins. Other unidentified proteins that associated with the SH3 domains of PCH family proteins may also play important roles in endocytosis.

Although the EFC domain alone was able to deform membrane in vitro, it is still unclear whether the EFC domain alone can deform plasma membrane into tubules in cells because the amount of dynamin-2 or N-WASP or the inhibition of actin polymerization

affects tubulation induced by the EFC domain (Fig. 9). Thus, it is possible that the EFC domain senses the curvature of endocytic vesicles for recruitment of N-WASP and dynamin-2. In this regard, it is interesting that the diameter of tubules induced by the EFC domain in vitro was larger than that induced by the amphiphysin BAR domain (Fig. 4 A; Peter et al., 2004). Differences in diameters may relate to differences in functions.

It has been reported that some PCH protein family members are involved in membrane-coupling processes, such as endocytosis, cell movement, and cytokinesis (Fankhauser et al., 1995; Qualmann and Kelly, 2000; Kessels and Qualmann, 2002; Kamioka et al., 2004; Chitu et al., 2005). Proteins containing the EFC domain may be involved in these shape changes involving both the membrane and cytoskeleton.

Materials and methods

Construct and protein expression

Human FBP17 complementary DNA (cDNA) was cloned in pEGFP-C1 (CLONTECH Laboratories, Inc.). Myc-tagged FBP17, Myc-tagged NH_2-terminal region deletion mutant (lacking 1–56 aa), and SH3 domain–deleted mutant (lacking 552–609 aa) were cloned in pEF-BOS plasmid vector. Human FBP17 (1–250, 1–300, 1–340, and 1–380 aa), mouse CIP4 (1–300 aa), FER (1–300 aa), PSTPIP1 (1–415 aa), PSTPIP2 (1–337 aa), BAR domain (1–286 aa) of amphiphysin2/Bin1, PH domain (130 aa) of PLCδ1, SH3 domains of FBP17 (553–609 aa), CIP4 (487–543 aa), Toca-1 (483–539 aa), and PSTPIP1 (362–415 aa) were obtained by RT-PCR. These sequences were confirmed, and then subcloned into pEGFP-C1 or pGEX vector (GE Healthcare). FBP17 (1–300 aa) were also subcloned into pCMV HA (CLONTECH Laboratories). The presence of GFP, Myc, and HA tag did not inhibit the tubulation of membrane in vivo. The pGEX-ENTH domain construct was made as described previously (Itoh et al., 2001). Mutagenesis was performed by PCR with mutated primers using Quikchange site-directed mutagenesis kit (Stratagene). Expression and purification of GST fusion proteins were performed using standard protocols. GST tag was cleaved from proteins by preScisson protease (GE Healthcare), but the presence of GST tag did not inhibit the binding or tubulation of liposomes.

Transfection, antibody, and immunofluorescence

COS-7 cells and A431 cells were cultured in DME containing 10% FCS. Transfection was performed using Lipofectamine 2000 (Invitrogen) according to the manufacturer's protocol. Transfected cells on coverslips were fixed in 3.7% formaldehyde for 15 min, permeabilized with 0.1% Triton X-100 for 5 min, and immunostained with various antibodies. Texas red–conjugated EGF (Invitrogen) uptake was examined as previously described (Itoh et al., 2001). Human EGF was purchased from Invitrogen. Polyclonal anti–N-WASP antibody was used as described previously (Fukuoka et al., 2001). Monoclonal anti-FLAG antibody and latrunculin B were obtained from Sigma-Aldrich. Monoclonal anti-Myc antibody, polyclonal anti-EGFR, and anti–dynamin-2 antibodies were obtained from Santa Cruz Biotechnologies, Inc. Monoclonal anti–dynamin-2 and anti-CIP4 were purchased from BD Biosciences. Polyclonal anti-GFP antibody was purchased from MBL International Corporation. For visualization of actin filaments, Alexa Fluor 647–conjugated phalloidin (Invitrogen) was incubated with fixed cells for 30 min. Secondary antibodies conjugated with Alexa Fluor 488, 568, and 647 were obtained from Invitrogen.

Liposome and lipid binding assay

Liposome binding assay was performed as described previously (Lee et al., 2002). Liposomes were prepared as follows. PE/PC liposomes consisted of PE (70%), PC (20%), and 10% PI or various phosphoinositides. Brain liposome was made of total bovine brain lipids (Folch fraction 1; Sigma-Aldrich). PE, PC, PS, and PI were obtained from Sigma-Aldrich. PI3P, PI4P, PI5P, PI(3,4)P2, PI(3,5)P2, and PI(3,4,5)P3 were purchased from Cell Signaling Technology. PI(4,5)P2 was obtained from Cell Signaling Technology and Echelon Bioscience, Inc. These lipid mixtures were resuspended at 1 mg/ml in 0.1 M sucrose, 20 mM Hepes, pH 7.4, 100 mM KCl, and 1 mM EDTA. To remove aggregated proteins, purified proteins were subjected to centrifugation at 70,000 rpm for 15 min at 4°C in a TL 100 rotor (Beckman Coulter). 5 μg of proteins were incubated with 100 μg of liposomes in 100 μl of buffer for 15 min at RT and centrifuged at 60,000 rpm for 15 min at 25°C. Supernatants and pellets were subjected to SDS-PAGE and stained with Coomassie brilliant blue. The intensity of protein bands was measured using Image J software (National Institutes of Health). Lipid overlay assay was performed using PIP strip membrane purchased from Echelon Biosciences, Inc. The interaction of the EFC domain with PI(4,5)P2 using a dual polarization interferometer was investigated with Analight Bio 200 (Farfield Sensors, Ltd.) as described previously (Oikawa et al., 2004). The K_d values were calculated from curve fitting.

In vitro liposome tubulation assay

Liposome tubulation assay was performed as previously described, with some modifications (Farsad et al., 2001). Liposomes containing 95% brain lipid and 5% rhodamine-conjugated PE (rhodamine-PE); or 85% brain lipid, 5% rhodamine-PE, and 10% of the indicated lipid; or 70% PE, 15% PC, 5% rhodamine-PE, and 10% of the indicated lipid were suspended in 0.3 M sucrose, and large liposomes (up to 3 μm in diameter) were formed by vortexing. 0.1 mg/ml of purified proteins were incubated with 0.2 mg/ml of liposomes in buffer (20 mM Hepes, pH 7.4, 100 mM KCl, and 1 mM EDTA) at RT for 2 min and immediately examined using confocal microscopy (Bio-Rad Laboratories). In vitro liposome tubulation assay was also performed by electron microscopy, as described previously (Farsad et al., 2001).

RNAi and RT-PCR

Stealth RNAi was purchased from Invitrogen. The siRNA sequence targeting as follows: FBP17, 5′-CCCACTTCATATGTCGAAGTCTGTT-3′; CIP4, 5′-GCAGTTGGAAGAACGCAGTCGTGAA-3′; Toca-1, 5′-GGCGCACAGAGTGTATGGTGAATTA-3′; and control random siRNA sequence, 5′-CCCTCGCACTGAGTCACCTTTGATT-3′. A431 cells were transfected with 10 μl of 20-μM siRNA and 4 μl of Oligofectamine reagent (Invitrogen) in a 6-well plate. After 24 h, a second transfection was performed, and the cells were cultured for 72 h and subjected to RT-PCR or various other experiments. The mRNA from RNAi-treated A431 cells was isolated using TRIZOL reagent (Invitrogen). A first-strand cDNA was synthesized from the mRNA by SuperScript first-strand synthesis system for RT-PCR (Invitrogen). The PCR amplification was performed using the first-strand cDNA. Amplification condition was as follows: 25 cycles of 30 s at 95°C, 30 s at 60°C, 60 s at 72°C, and a final extension of 10 min at 72°C.

In vitro actin polymerization assay

Actin was prepared from rabbit skeletal muscle and monomeric actin was purified using gel filtration on Superdex 200 (GE Healthcare) in G buffer (2 mM Tris-HCl, pH 8.0, 0.2 mM $CaCl_2$, 0.5 mM DTT, and 0.2 mM ATP). Purified actin was labeled with N-(1-pyrene) iodoacetamide (Invitrogen). Purification of Arp2/3 complex and N-WASP and in vitro actin polymerization assay were performed as described previously (Fukuoka et al., 2001).

Quantification of EGF internalization

EGF endocytosis assays using biotinylated EGF were performed as described previously (Vieira et al., 1996), but with modifications. A431 cells were treated with siRNA as described in RNAi and RT-PCR. After 72 h, cells were starved with serum-free DME for 16 h. Cells were then incubated with 20 ng/ml of biotinylated EGF (Invitrogen) for 30 min at 4°C and moved to a 37°C incubator for the indicated times. To measure internalized EGF, cells were washed two times with ice-cold acid buffer (10 mM HCl and 150 mM NaCl, pH 2.0) to remove surface-bound EGF. To measure total bound EGF, cells were washed two times with ice-cold PBS instead of the acid wash. Cells were lysed in PBS containing 1% Triton X-100. Cell lysates were incubated with an ELISA plate coated with anti-EGF antibody (polyclonal; Abcam plc) at RT for 1 h. After being washed with PBS containing 0.05% Tween 20, the plate was incubated with streptavidin-peroxidase (Sigma-Aldrich) at RT for 30 min and bound, and biotinylated EGF was detected by reaction with its substrate, orthophenyl enediamine dihydrochloride. The absorbance was measured at 492 nm in an ELISA plate reader (Bio-Rad Laboratories).

Image acquisition and processing

All photographic images were taken through a microscope (ECLIPSE E600; Nikon) with a confocal microscopy system (Radiance 2000; Bio-Rad Laboratories) at RT. Fluorochromes used include Alexa Fluor 488, 546, and 647 or rhodamine-labeled phalloidin (all Invitrogen). A 60× oil immersion objective, NA 1.40 (Nikon) was used. Images were assembled with Photoshop (Adobe). In each plate, photographs were cropped and each fluorochrome was adjusted identically for brightness and contrast to represent the observed images.

Western blotting, GST pull-down, immunoprecipitation, and densitometry

The samples were electrophoresed in SDS-PAGE gels, stained with Coomassie brilliant blue, or transferred to polyvinylidene difluoride membrane, blocked with 5% nonfat dry milk in PBS and 0.1% Tween 20, incubated with primary antibodies, and then incubated with alkaline phosphatase–conjugated goat immunoglobulin secondary antibodies (Promega), followed by incubation with NBT/BCIP substrate (Roche). GST pull-down assay and immunoprecipitation were described previously (Fukuoka et al., 2001). Resulting gels or blots were scanned with a calibrated densitometer (model GS-710; Bio-Rad Laboratories) and quantified with Image J software.

Online supplemental material

Fig. S1 shows an alignment of EFC and BAR domains. Fig. S2 shows colocalization between FBP17 and dynamin-2 or EGF at the plasma membrane. Fig. S3 shows a possible mechanism of involvement of FBP17 in EGFR internalization. Online supplemental material is available at http://www.jcb.org/cgi/content/full/jcb.200508091/DC1.

We thank the members of the Takenawa lab for technical support and valuable discussions.

This work was supported in part by a grant-in-aid for Cancer Research from the Ministry of Education, Culture, Sports, Science, and Technology of Japan.

Submitted: 12 August 2005
Accepted: 13 December 2005

References

Aspenstrom, P. 1997. A Cdc42 target protein with homology to the non-kinase domain of FER has a potential role in regulating the actin cytoskeleton. *Curr. Biol.* 7:479–487.

Cao, H., J.D. Orth, J. Chen, S.G. Weller, J.E. Heuser, and M.A. McNiven. 2003. Cortactin is a component of clathrin-coated pits and participates in receptor-mediated endocytosis. *Mol. Cell. Biol.* 23:2162–2170.

Chitu, V., F.J. Pixley, F. Macaluso, D.R. Larson, J. Condeelis, Y.G. Yeung, and E.R. Stanley. 2005. The PCH family member MAYP/PSTPIP2 directly regulates F-actin bundling and enhances filopodia formation and motility in macrophages. *Mol. Biol. Cell*. 16:2947–2959.

Engqvist-Goldstein, A.E., and D.G. Drubin. 2003. Actin assembly and endocytosis: from yeast to mammals. *Annu. Rev. Cell Dev. Biol.* 19:287–332.

Fankhauser, C., A. Reymond, L. Cerutti, S. Utzig, K. Hofmann, and V. Simanis. 1995. The *S. pombe* cdc15 gene is a key element in the reorganization of F-actin at mitosis. *Cell*. 82:435–444.

Farsad, K., N. Ringstad, K. Takei, S.R. Floyd, K. Rose, and P. De Camilli. 2001. Generation of high curvature membranes mediated by direct endophilin bilayer interactions. *J. Cell Biol.* 155:193–200.

Ford, M.G., I.G. Mills, B.J. Peter, Y. Vallis, G.J. Praefcke, P.R. Evans, and H.T. McMahon. 2002. Curvature of clathrin-coated pits driven by epsin. *Nature*. 419:361–366.

Fukuoka, M., S. Suetsugu, H. Miki, K. Fukami, T. Endo, and T. Takenawa. 2001. A novel neural Wiskott-Aldrich syndrome protein (N-WASP) binding protein, WISH, induces Arp2/3 complex activation independent of Cdc42. *J. Cell Biol.* 152:471–482.

Hinshaw, J.E. 2000. Dynamin and its role in membrane fission. *Annu. Rev. Cell Dev. Biol.* 16:483–519.

Ho, H.Y., R. Rohatgi, A.M. Lebensohn, L. Ma, J. Li, S.P. Gygi, and M.W. Kirschner. 2004. Toca-1 mediates Cdc42-dependent actin nucleation by activating the N-WASP-WIP complex. *Cell*. 118:203–216.

Hussain, N.K., S. Jenna, M. Glogauer, C.C. Quinn, S. Wasiak, M. Guipponi, S.E. Antonarakis, B.K. Kay, T.P. Stossel, N. Lamarche-Vane, and P.S. McPherson. 2001. Endocytic protein intersectin-l regulates actin assembly via Cdc42 and N-WASP. *Nat. Cell Biol.* 3:927–932.

Itoh, T., S. Koshiba, T. Kigawa, A. Kikuchi, S. Yokoyama, and T. Takenawa. 2001. Role of the ENTH domain in phosphatidylinositol-4,5-bisphosphate binding and endocytosis. *Science*. 291:1047–1051.

Kakimoto, T., H. Katoh, and M. Negishi. 2004. Identification of splicing variants of Rapostlin, a novel RND2 effector that interacts with neural Wiskott-Aldrich syndrome protein and induces neurite branching. *J. Biol. Chem.* 279:14104–14110.

Kaksonen, M., Y. Sun, and D.G. Drubin. 2003. A pathway for association of receptors, adaptors, and actin during endocytic internalization. *Cell*. 115:475–487.

Kamioka, Y., S. Fukuhara, H. Sawa, K. Nagashima, M. Masuda, M. Matsuda, and N. Mochizuki. 2004. A novel dynamin-associating molecule, formin-binding protein induces tubular membrane invaginations and participates in endocytosis. *J. Biol. Chem.* 279:40091–40099.

Kessels, M.M., and B. Qualmann. 2002. Syndapins integrate N-WASP in receptor-mediated endocytosis. *EMBO J.* 21:6083–6094.

Kessels, M.M., A.E. Engqvist-Goldstein, D.G. Drubin, and B. Qualmann. 2001. Mammalian Abp1, a signal-responsive F-actin–binding protein, links the actin cytoskeleton to endocytosis via the GTPase dynamin. *J. Cell Biol.* 153:351–366.

Lee, E., M. Marcucci, L. Daniell, M. Pypaert, O.A. Weisz, G.C. Ochoa, K. Farsad, M.R. Wenk, and P. De Camilli. 2002. Amphiphysin 2 (Bin1) and T-tubule biogenesis in muscle. *Science*. 297:1193–1196.

Lippincott, J., and R. Li. 2000. Involvement of PCH family proteins in cytokinesis and actin distribution. *Microsc. Res. Tech.* 49:168–172.

Merrifield, C.J., M.E. Feldman, L. Wan, and W. Almers. 2002. Imaging actin and dynamin recruitment during invagination of single clathrin-coated pits. *Nat. Cell Biol.* 4:691–698.

Merrifield, C.J., B. Qualmann, M.M. Kessels, and W. Almers. 2004. Neural Wiskott Aldrich Syndrom protein (N-WASP) and the Arp2/3 complex are recruited to sites of clathrin-mediated endocytosis in cultured fibroblasts. *Eur. J. Cell Biol.* 83:13–18.

Merrifield, C.J., D. Perrais, and D. Zenisek. 2005. Coupling between clathrin-coated-pit invagination, cortactin recruitment, and membrane scission observed in live cells. *Cell*. 121:593–606.

Modregger, J., B. Ritter, B. Witter, M. Paulsson, and M. Plomann. 2000. All three PACSIN isoforms bind to endocytic proteins and inhibit endocytosis. *J. Cell Sci.* 113:4511–4521.

Munn, A.L. 2001. Molecular requirements for the internalisation step of endocytosis: insights from yeast. *Biochim. Biophys. Acta*. 1535:236–257.

Oikawa, T., H. Yamaguch, T. Itoh, M. Kato, T. Ijuin, D. Yamazaki, S. Suetsugu, and T. Takenawa. 2004. PtdIns(3,4,5)P3 binding is necessary for WAVE2-induced formation of lamellipodia. *Nat. Cell Biol.* 6:420–426.

Otsuki, M., T. Itoh, and T. Takenawa. 2003. Neural Wiskott-Aldrich syndrome protein is recruited to rafts and associates with endophilin A in response to epidermal growth factor. *J. Biol. Chem.* 278:6461–6469.

Peter, B.J., H.M. Kent, I.G. Mills, Y. Vallis, P.J. Butler, P.R. Evans, and H.T. McMahon. 2004. BAR domains as sensors of membrane curvature: the amphiphysin BAR structure. *Science*. 303:495–499.

Pollard, T.D., and G.G. Borisy. 2003. Cellular motility driven by assembly and disassembly of actin filaments. *Cell*. 112:453–465.

Praefcke, G.J., and H.T. McMahon. 2004. The dynamin superfamily: universal membrane tubulation and fission molecules? *Nat. Rev. Mol. Cell Biol.* 5:133–147.

Qualmann, B., and R.B. Kelly. 2000. Syndapin isoforms participate in receptor-mediated endocytosis and actin organization. *J. Cell Biol.* 148:1047–1062.

Qualmann, B., M.M. Kessels, and R.B. Kelly. 2000. Molecular links between endocytosis and the actin cytoskeleton. *J. Cell Biol.* 150:F111–F116.

Razzaq, A., I.M. Robinson, H.T. McMahon, J.N. Skepper, Y. Su, A.C. Zelhof, A.P. Jackson, N.J. Gay, and C.J. O'Kane. 2001. Amphiphysin is necessary for organization of the excitation-contraction coupling machinery of muscles, but not for synaptic vesicle endocytosis in *Drosophila*. *Genes Dev.* 15:2967–2979.

Rodriguez, O.C., A.W. Schaefer, C.A. Mandato, P. Forscher, W.M. Bement, and C.M. Waterman-Storer. 2003. Conserved microtubule-actin interactions in cell movement and morphogenesis. *Nat. Cell Biol.* 5:599–609.

Schafer, D.A. 2002. Coupling actin dynamics and membrane dynamics during endocytosis. *Curr. Opin. Cell Biol.* 14:76–81.

Spencer, S., D. Dowbenko, J. Cheng, W. Li, J. Brush, S. Utzig, V. Simanis, and L.A. Lasky. 1997. PSTPIP: a tyrosine phosphorylated cleavage furrow–associated protein that is a substrate for a PEST tyrosine phosphatase. *J. Cell Biol.* 138:845–860.

Takei, K., V. Haucke, V. Slepnev, K. Farsad, M. Salazar, H. Chen, and P. De Camilli. 1998. Generation of coated intermediates of clathrin-mediated endocytosis on protein-free liposomes. *Cell*. 94:131–141.

Takei, K., V. Haucke, V. Slepnev, M. Salazar, H. Chen, and P. De Camilli. 1999. Functional partnership between amphiphysin and dynamin in clathrin-mediated endocytosis. *Nat. Cell Biol.* 1:133–139.

Thompson, J.D., T.J. Gibson, F. Plewniak, F. Jeanmougin, and D.G. Higgins. 1997. The CLUSTAL_X windows interface: flexible strategies for multiple sequence alignment aided by quality analysis tools. *Nucleic Acids Res.* 25:4876–4882.

Vieira, A.V., C. Lamaze, and S.L. Schmid. 1996. Control of EGF receptor signaling by clathrin-mediated endocytosis. *Science*. 274:2086–2089.

Yarar, D., C.M. Waterman-Storer, and S.L. Schmid. 2005. A dynamic actin cytoskeleton functions at multiple stages of clathrin-mediated endocytosis. *Mol. Biol. Cell*. 16:964–975.

Zerial, M., and H. McBride. 2001. Rab proteins as membrane organizers. *Nat. Rev. Mol. Cell Biol.* 2:107–117.